


Flat bands promoted by Hund's rule coupling in the candidate double-layer high-temperature superconductor $\text{La}_3\text{Ni}_2\text{O}_7$ under high pressure

Yingying Cao^{1,2} and Yi-feng Yang^{1,2,3,*}

¹Beijing National Laboratory for Condensed Matter Physics and Institute of Physics, Chinese Academy of Sciences, Beijing 100190, China

²University of Chinese Academy of Sciences, Beijing 100049, China

³Songshan Lake Materials Laboratory, Dongguan, Guangdong 523808, China

 (Received 15 July 2023; revised 8 January 2024; accepted 9 January 2024; published 8 February 2024)

Experiments in the high-temperature superconductor $\text{La}_3\text{Ni}_2\text{O}_7$ have revealed both high T_c and strange metal behaviors over a wide pressure range. While first-principles density functional theory has predicted weakly correlated bands that cannot explain these key observations, we report here strongly correlated electronic band structure calculations that reveal the dual nature of Ni- d electrons with almost localized d_{z^2} orbitals due to on-site Coulomb repulsion and flat bands of Ni- $d_{x^2-y^2}$ and Ni- d_{z^2} quasiparticles near the Fermi energy. We find that the quasiparticle effective masses are greatly enhanced by Hund's rule coupling and their lifetimes are inversely proportional to temperature, which explains the experimentally observed strange metal behavior in the normal state. Our calculations also reveal strong antiferromagnetic spin correlations of Ni- d electrons, which may provide the pairing force of quasiparticles for high-temperature superconductivity. The presence of flat bands and the interplay of orbital-selective Mott, Hund, and Kondo physics lay the basis for a two-component theory of its pairing mechanism and make $\text{La}_3\text{Ni}_2\text{O}_7$ a unique platform for exploring rich emergent quantum many-body phenomena in the future.

DOI: [10.1103/PhysRevB.109.L081105](https://doi.org/10.1103/PhysRevB.109.L081105)

The recent discovery of possible high-temperature superconductivity in the pressurized Ruddlesden-Popper perovskite $\text{La}_3\text{Ni}_2\text{O}_7$ [1] has stimulated intensive investigations on its fundamental electronic structures and potential pairing mechanism [2–11]. The Ni cation is expected to have a valence of +2.5. First-principles calculations yield an almost fully filled Ni- d_{z^2} bonding state and quarter-filled Ni- $d_{x^2-y^2}$ bands due to the double-layer structure [1,12], suggesting a weak correlation picture different from the cuprate high-temperature superconductors and the infinite-layer nickelate superconductors, in which the transition metal ions (Cu^{2+} or Ni^{1+}) have a d^9 configuration with (almost) half-filled and localized $d_{x^2-y^2}$ orbitals due to Mott localization [13–17]. Questions arise on how the weakly correlated bands in $\text{La}_3\text{Ni}_2\text{O}_7$ can support the experimentally observed high-temperature superconductivity around 80 K [1]. While several studies focus on the electronic correlation of $\text{La}_3\text{Ni}_2\text{O}_7$ [5,10], it appears that the renormalization factor of the Ni- d_{z^2} orbital changes from 3 to 6 as the interaction parameter U varies from 6 to 10 eV. Electronic features which are of primary importance for its Cooper pairing and the strange metal behavior observed in the normal state are not fully clarified yet [1].

In this Letter, we show a strong correlation picture for superconducting $\text{La}_3\text{Ni}_2\text{O}_7$ by performing a systematic investigation of its strongly correlated electronic band structures using density functional theory (DFT) [18,19] combined with dynamical mean-field theory (DMFT) [20–25] as present in

the EDMFT package developed by Haule [25]. Our calculations reveal an itinerant-localized duality of strongly correlated d_{z^2} electrons with both quasiparticle bands and local moment fluctuations. The $d_{x^2-y^2}$ bands are also strongly renormalized near the Fermi energy by hybridizing with the d_{z^2} bands. These differ distinctively from a pure DFT prediction but resemble those in orbital-selective Mott systems or Kondo lattice systems [26–29]. Hund's rule coupling, enhancing greatly the quasiparticle effective mass, rather than Hubbard U , is found to compete with the hybridization, causing very flat bands near the Fermi energy. Our self-energy analyses yield quasiparticle lifetimes inversely proportional to temperature, which explains the strange metal behavior observed in the normal state resistivity [1]. Static local spin susceptibility follows typical Curie-Weiss behavior, confirming the presence of d_{z^2} local moments, and gives a large antiferromagnetic coupling possibly from their interlayer superexchange interaction through the apical $O-p_z$ orbitals. These imply that the Cooper pairing might be primarily induced by the antiferromagnetic spin coupling of the almost localized d_{z^2} electrons and become coherent through hybridization (and self-doping) with $d_{x^2-y^2}$ electrons. This provides a basis for the high-temperature superconductivity in the double-layer nickelate $\text{La}_3\text{Ni}_2\text{O}_7$ that may differ from the cuprates [13]. Our work explains two key experimental observations underlying the basic physics of $\text{La}_3\text{Ni}_2\text{O}_7$.

Superconducting $\text{La}_3\text{Ni}_2\text{O}_7$ has an orthorhombic structure with the space group $Fmmm$. As shown in Fig. 1(a), each Ni ion is surrounded by six O ions to form an octahedron, producing a double-layer structure with two Ni ions sharing an apical O. For later comparison, Fig. 1(b) gives the DFT

*yifeng@iphy.ac.cn

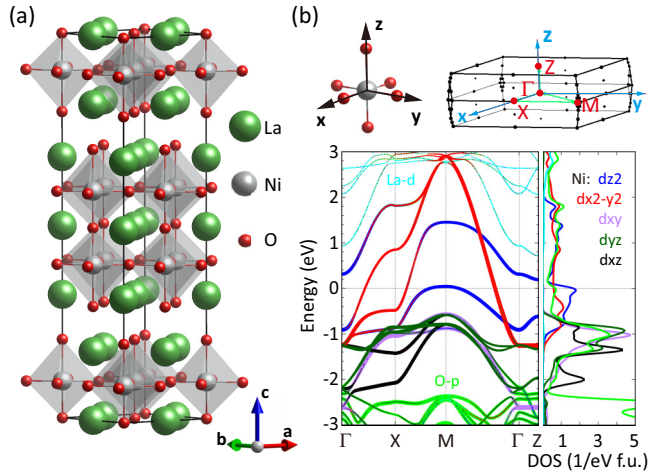


FIG. 1. (a) High-pressure crystal structure of the candidate high-temperature superconductor $\text{La}_3\text{Ni}_2\text{O}_7$ visualized by VESTA [30]. (b) Orbital-projected band structures and densities of states for Ni- d , O- p , and La- d calculated by DFT at 29.5 GPa, with optimized structural parameters based on experiment [1]. The paths are shown as green lines in the schematic diagram of the Brillouin zone plotted using XCRYSDEN [31], where the local z axis points along the c direction and the x and y axes along the Ni-O bonds in the ab plane. The red points mark the high-symmetry points in the Brillouin zone.

band structures calculated using WIEN2K [19,32]. The overall results are similar to those reported in previous DFT calculations [1]. We obtain a metal with three bands crossing the Fermi level. These bands are primarily from Ni- d_{z^2} and Ni- $d_{x^2-y^2}$ orbitals but contain substantial contributions from O- p orbitals. The Ni- $d_{x^2-y^2}$ bands (red) have a large bandwidth of about 4 eV and are strongly hybridized with d_{z^2} . The d_{z^2} orbitals split into bonding and antibonding states due to strong interlayer coupling through the apical O- p_z orbital, giving rise to two bands (blue) with a typical bandwidth of 1 eV separated by about 1.4 eV around M . The bonding state is almost fully occupied, while the antibonding state is above the Fermi energy and considered irrelevant in previous studies, which leads to an effective low-energy model with an almost fully filled d_{z^2} bonding band and two quarter-filled $d_{x^2-y^2}$ bands. We will see that this DFT picture is insufficient due to the strong electronic correlations of Ni- d electrons. In particular, the doubly occupied d_{z^2} bonding state will be replaced by almost localized d_{z^2} electrons on each Ni ion and flat quasiparticle bands due to their hybridization and Hund's rule coupling with more itinerant $d_{x^2-y^2}$ electrons. Pressurized $\text{La}_3\text{Ni}_2\text{O}_7$ is therefore a unique system with peculiar orbital-selective Mott, Hund, and Kondo physics.

To construct the DMFT Hamiltonian, we employed the Kohn-Sham bands within the energy window from -10 to 10 eV with respect to the Fermi energy. The density-density interaction was incorporated among the Ni- d_{z^2} , $d_{x^2-y^2}$, d_{xy} , d_{xz} , and d_{yz} orbitals to account for the electronic correlations. A full potential interaction was also tested and shows no qualitative differences in the electronic structure compared to the density-density interaction. The values of U and J were chosen according to previous studies on infinite-layer nickelates and perovskite nickelates [33,34]. We took the hybridization

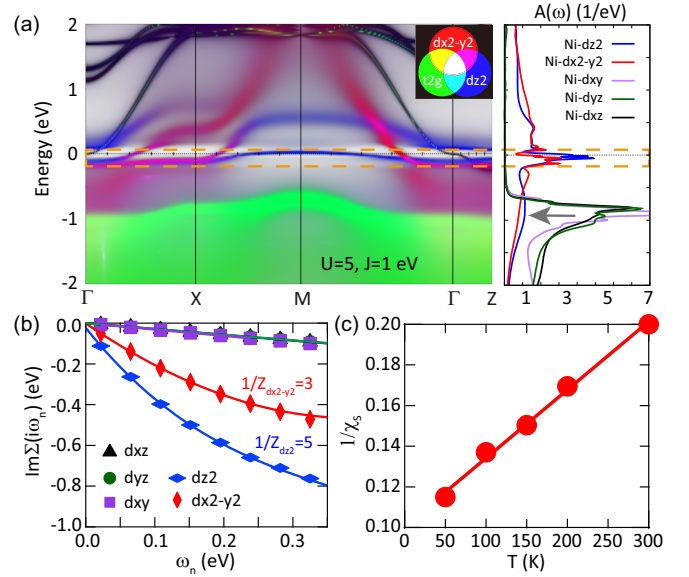


FIG. 2. (a) Orbital-projected spectral function of Ni- d electrons calculated using DFT+DMFT for $U = 5$ eV and $J = 1$ eV at 80 K. The red color is assigned to $d_{x^2-y^2}$, blue to d_{z^2} , and green to t_{2g} . Also shown are the corresponding momentum-integrated densities of states, with the three orbital components of t_{2g} being separated. The orange box highlights the peak from the flat quasiparticle bands of the almost localized d_{z^2} orbitals. The gray arrow highlights the lower Hubbard band of Ni- d_{z^2} . The $d_{x^2-y^2}$ orbital shows similar features in the density of states due to its strong hybridization with the d_{z^2} orbital. (b) Imaginary part of the orbital-dependent self-energy for $U = 5$ eV and $J = 1$ eV at 80 K. The solid lines are fittings to the data using the fourth-order polynomial, giving an inverse renormalization factor of 5 for d_{z^2} and 3 for $d_{x^2-y^2}$ at the Fermi energy. (c) Temperature dependence of the inverse static local spin susceptibility $1/\chi_s$. The solid line marks a linear-in-temperature fit according to the Curie-Weiss law.

expansion continuous-time quantum Monte Carlo approach as the DMFT impurity solver [35]. To achieve high accuracy, more than 3×10^7 Monte Carlo steps were performed on each of the 56 processors. The spectral function was obtained by using the maximum entropy method for the analytic continuation of the self-energy [36]. The double counting in DFT+DMFT was treated using the nominal scheme [25] with the Ni- d occupation of 7.5, as derived from the valence $+2.5$ of Ni ions indicated by both DFT and x-ray photoemission spectroscopy measurements [11]. We have explored other double-counting schemes [37,38], and not surprisingly, found the Ni- d occupation varies a lot from 5.2 to 8.6. Among them, only the nominal scheme yields a value of 7.67, in agreement with the $\text{Ni}^{2.5+}$ state, while the exact double-counting scheme gives an occupation of about 8.1. We therefore decided to choose the nominal scheme for the study of $\text{La}_3\text{Ni}_2\text{O}_7$ in this work.

Figure 2(a) plots our DFT+DMFT spectral function calculated at 80 K with the on-site Coulomb repulsion $U = 5$ eV and Hund's rule coupling $J = 1$ eV on the Ni- d electrons. Compared to DFT, the bonding-antibonding splitting is greatly reduced. The Ni- d_{z^2} quasiparticle band around M is also strongly renormalized and becomes very flat near

the Fermi energy. Its bandwidth is only about 0.2 eV, a factor of 5 narrower than the DFT prediction. The exact value of band renormalization derived from $Z^{-1} = 1 - \partial \text{Im} \Sigma(i\omega)/\partial \omega|_{\omega \rightarrow 0^+}$ by fitting the lowest six points of the imaginary part of the orbital-dependent self-energy with a fourth-order polynomial [39] is shown in Fig. 2(b). We find a mass enhancement of 5 for the Ni- d_{z^2} quasiparticles, consistent with its reduced bandwidth from about 1 to 0.2 eV.

Interestingly, the Ni- $d_{x^2-y^2}$ electrons also have a large mass enhancement of 3. This seems odd because the $d_{x^2-y^2}$ bands are quarter filled and far away from the Mott regime. We notice that in the band plot as shown in Fig. 2(a), this large renormalization only occurs near the Fermi energy, where $d_{x^2-y^2}$ hybridizes strongly with d_{z^2} and produces some quite flat bands (Γ -X) with both orbital characters. Away from the Fermi energy, the $d_{x^2-y^2}$ bands are less renormalized, with the top at about 2.5 eV compared to 3 eV in DFT. Thus, the large renormalization of $d_{x^2-y^2}$ electrons near the Fermi energy mainly originates from their hybridization with d_{z^2} , as is also confirmed from the similar peak structures in their densities of states. This peculiar hybridization feature is close to those in heavy fermion systems [28,29], where the conduction bands are only bent near the Fermi energy due to the Kondo hybridization with localized orbitals. On the other hand, because the atomic wave functions of Ni- d_{z^2} and Ni- $d_{x^2-y^2}$ orbitals are orthogonal, their hybridization in $\text{La}_3\text{Ni}_2\text{O}_7$ should mostly occur from the hopping between neighboring Ni sites through the O- p orbitals.

Connections to the Kondo or orbital-selective Mott physics are further supported by the almost localized behavior of d_{z^2} electrons. Different from previous studies, we see in Fig. 2(a) the blurred lower Hubbard band below the Fermi energy, as also marked by the arrow at around -1 eV in the orbital-resolved densities of states. This localized spectral weight indicates the dual nature of strongly correlated Ni- d_{z^2} electrons. To confirm it, we further calculate the static local spin susceptibility χ_s of Ni- d electrons as a function of temperature. As shown in Fig. 2(c), its inverse follows nicely the Curie-Weiss law (the straight line), which confirms the presence of well-defined local moments on Ni ions. The linear extrapolation gives a large Weiss temperature of approximately -300 K, indicating strong antiferromagnetic spin correlations among Ni- d electrons. Since Hund's rule coupling between d_{z^2} and $d_{x^2-y^2}$ electrons is ferromagnetic, the large antiferromagnetic correlations should mostly arise from the interlayer superexchange coupling between two Ni- d_{z^2} spins through the apical O- p_z orbital. In cuprates, the superexchange interaction between localized Cu- $d_{x^2-y^2}$ spins gives the basic magnetic energy scale for the Cooper pairing. One may speculate that the superexchange mechanism also plays a similar role here in superconducting $\text{La}_3\text{Ni}_2\text{O}_7$.

Due to the multiorbital nature, Hund's rule coupling between d_{z^2} and $d_{x^2-y^2}$ orbitals could be also important. To see its effect, we compare in Fig. 3(a) the calculated spectral function for $U = 5$ eV and $J = 0$. Quite unexpectedly, the Ni- d_{z^2} bands become much broader (0.7 eV), and the $d_{x^2-y^2}$ bandwidth increases to about 3 eV, which is close to the DFT value. It seems that Hund's rule coupling plays an important role in the renormalization. For clarification, we plot the renormalization factor $1/Z$ as functions of U and J at 300 K in Figs. 3(b)

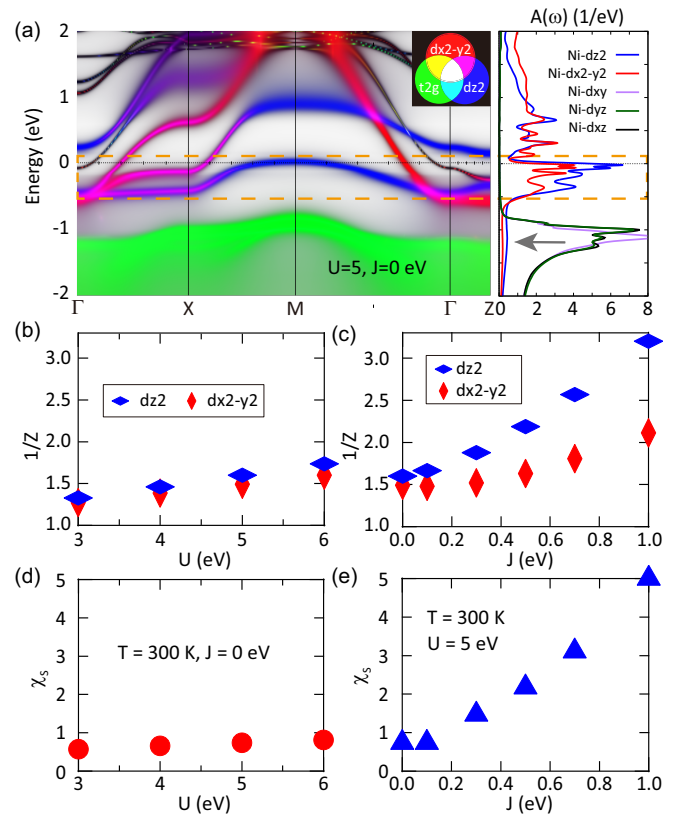


FIG. 3. (a) Orbital-projected spectral function and corresponding densities of states of Ni- d electrons calculated using DFT+DMFT for $U = 5$ eV and $J = 0$ eV at 80 K, plotted as in Fig. 2(a) showing reduced band renormalization. (b), (c) Inverse renormalization factor of Ni- d_{z^2} and Ni- $d_{x^2-y^2}$ orbitals extracted from the self-energy at 300 K as functions of the Coulomb repulsion U for $J = 0$ and of Hund's rule coupling J for $U = 5$ eV, respectively. (d), (e) The static local spin susceptibility χ_s as functions of U for $J = 0$ and of J for $U = 5$ eV, respectively.

and 3(c). Contrary to the usual expectation, for $J = 0$, $1/Z$ varies only slightly from 1.3 to 1.7 as U increases from 3 to 6 eV and is almost the same for two orbitals. But if we fix $U = 5$ eV and increase J from 0 to 1 eV, the inverse renormalization factor increases rapidly from about 1.6 to 3.2 for d_{z^2} and 1.5 to 2.1 for $d_{x^2-y^2}$. Thus, Hund's rule coupling greatly enhances the quasiparticle renormalization and promotes the flat bands near the Fermi energy. It also induces a large difference in their orbital dependence. As a result, the Ni- d_{z^2} band becomes noticeably more flattened with increasingly J . These are characteristic features of the Hund metal analog to iron-based superconductors [40,41], given the small variation of Hund's rule coupling compared to the Hubbard interaction U . Hund's coupling in infinite-layer nickelates has been emphasized [42,43]. It leads to a very different minimal model by selecting which orbital is to be doped. Here, it could be that ferromagnetic Hund's rule coupling tends to compete with the Kondo hybridization, thus reducing the effective Kondo energy scale that determines the quasiparticle bandwidth. Figures 3(d) and 3(e) confirm this idea by showing the static local spin susceptibility as functions of U and J , which grows significantly at large J , reflecting enhanced local

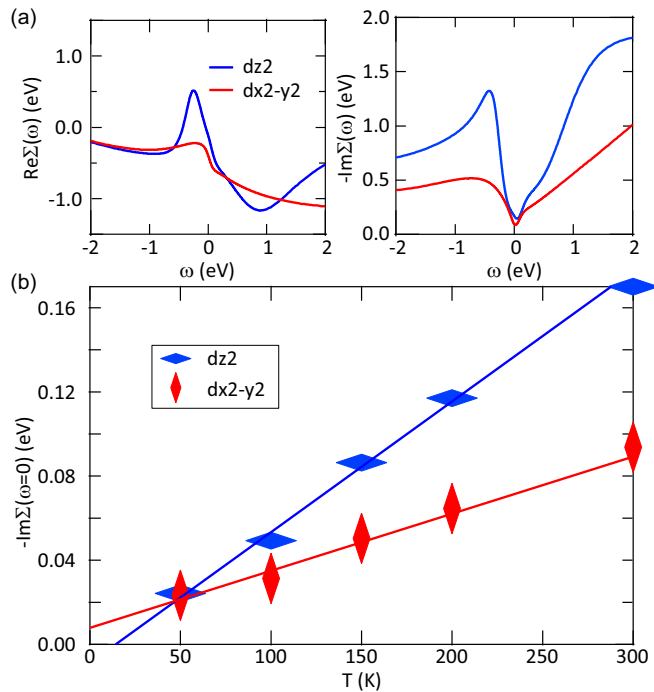


FIG. 4. (a) Typical results for the real and imaginary parts of the orbital-dependent self-energy for d_{z^2} (blue) and $d_{x^2-y^2}$ (red) orbitals in real frequency obtained using the maximum entropy method. (b) Temperature dependence of the imaginary part of the self-energy at zero frequency, $-\text{Im}\Sigma(\omega=0)$, calculated using DFT+DMFT for $U = 5$ eV and $J = 1$ eV. The solid line is a linear-in-temperature fit, showing strange metal behavior as observed in the resistivity measurement above the superconducting transition temperature.

moment fluctuations due to the suppression of hybridization. Given the important role of Hund's rule coupling in understanding the low-energy physics of $\text{La}_3\text{Ni}_2\text{O}_7$, it would be beneficial to determine its value through both first-principles calculations and experiments.

Taken together, there appears to be an intimate interplay of orbital-selective Mott localization, Kondo hybridization, and Hund physics in superconducting $\text{La}_3\text{Ni}_2\text{O}_7$. The dual property of Ni- d_{z^2} electrons is a characteristic feature of strongly correlated orbitals in Mott or Kondo systems. Since the d_{z^2} orbitals are perpendicular to the ab plane, their in-plane hopping is relatively small. Thus for double-layer $\text{La}_3\text{Ni}_2\text{O}_7$, one may consider to start from Mott-localized d_{z^2} electrons with a large interlayer superexchange interaction, and explore their delocalization by hopping to neighboring Ni- $d_{x^2-y^2}$ orbitals. Their hybridization has two effects. It may not only create hybridization bands (Γ - X) near the Fermi energy as in Kondo lattice systems, but also produce self-doping to the localized d_{z^2} orbitals as in the hole-doped cuprates, causing a d_{z^2} quasiparticle band around M whose position depends on the interlayer hopping. Hund's rule coupling may compete with hybridization and greatly promote band flatness. These results are distinctively different from the DFT weak correlation picture with an almost fully occupied d_{z^2} bonding band. The possibility of Mott physics with strong renormalization has been confirmed in the latest optical measurements at ambient pressure [44].

Our strong correlation picture derived from the above DFT+DMFT calculations has important implications for understanding two major experimental observations in pressurized $\text{La}_3\text{Ni}_2\text{O}_7$, namely its strange metallicity in the normal state and its high-temperature superconductivity below around 80 K. To see how the linear-in-temperature resistivity may arise in our picture, we show in Fig. 4 the self-energy $\Sigma(\omega)$ for both d_{z^2} and $d_{x^2-y^2}$ orbitals in real frequency. The imaginary part of the self-energy at zero frequency gives the inverse of the corresponding quasiparticle lifetimes at the Fermi energy. Their temperature dependencies are given in Fig. 4(b) up to 300 K. We find both can be well fitted using the linear-in-temperature function (solid lines). This gives a quasiparticle lifetime inversely proportional to the temperature, which is often used as an indicator of strange metallicity in the literature [45]. Our results suggest that the strange metal behavior observed in $\text{La}_3\text{Ni}_2\text{O}_7$ comes from the flat quasiparticle bands around the Fermi energy due to strong electronic correlations.

Naturally, superconductivity born out of this strange metallic normal state should also originate from the pairing of strongly correlated d_{z^2} and $d_{x^2-y^2}$ electrons, potentially mediated by an antiferromagnetic spin interaction as revealed in our susceptibility calculations. It is possible that the large antiferromagnetic superexchange coupling between Ni- d_{z^2} electrons may first lead to interlayer preformed pairs [46,47], which eventually give rise to high-temperature superconductivity when phase coherence is established as the hybridization with the $d_{x^2-y^2}$ orbitals increases [48]. This two-component scenario has been supported by our Monte Carlo simulations for the above strongly correlated model [49]. It will be interesting to see if a pseudogap might also exist in this system as is present in the cuprates [50,51].

To summarize, we have performed systematic DFT+DMFT studies of the strongly correlated electronic band structures of superconducting $\text{La}_3\text{Ni}_2\text{O}_7$ under high pressure. Our analyses reveal some key features in the electronic and magnetic properties, including almost localized d_{z^2} electrons, very flat d_{z^2} quasiparticle bands, and strongly renormalized $d_{x^2-y^2}$ - d_{z^2} hybridized bands. We explain the normal state strange metal behavior from the linear-in-temperature dependence of the inverse quasiparticle lifetimes and find strong antiferromagnetic spin correlations that may be responsible for their Cooper pairing. Our observation of flat-band features, driven by the interplay of orbital-selective Mott, Hund, and Kondo physics, confirms the peculiarity of double-layer $\text{La}_3\text{Ni}_2\text{O}_7$, and establishes a strong correlation picture for its possible high-temperature superconductivity. The coexistence of these competing mechanisms may give rise to even richer correlated many-body phenomena to be explored in future theoretical and experimental studies.

This work was supported by the National Natural Science Foundation of China (Grants No. 11974397 and No. 12174429) and the Strategic Priority Research Program of the Chinese Academy of Sciences (Grant No. XDB33010100). We thank G.-M. Zhang for discussions and the Tianhe platforms at the National Supercomputer Center in Tianjin for technical support.

- [1] H. Sun, M. Huo, X. Hu, J. Li, Y. Han, L. Tang, Z. Mao, P. Yang, B. Wang, J. Cheng, D.-X. Yao, G.-M. Zhang, and M. Wang, Signatures of superconductivity near 80 K in a nickelate under high pressure, *Nature (London)* **621**, 493 (2023).
- [2] Z. Luo, X. Hu, M. Wang, W. Wú, and D.-X. Yao, Bilayer two-orbital model of $\text{La}_3\text{Ni}_2\text{O}_7$ under pressure, *Phys. Rev. Lett.* **131**, 126001 (2023).
- [3] Y. Zhang, L.-F. Lin, A. Moreo, and E. Dagotto, Electronic structure, dimer physics, orbital-selective behavior, and magnetic tendencies in the bilayer nickelate superconductor $\text{La}_3\text{Ni}_2\text{O}_7$ under pressure, *Phys. Rev. B* **108**, L180510 (2023).
- [4] Q.-G. Yang, D. Wang, and Q.-H. Wang, Possible s_{\pm} -wave superconductivity in $\text{La}_3\text{Ni}_2\text{O}_7$, *Phys. Rev. B* **108**, L140505 (2023).
- [5] F. Lechermann, J. Gondolf, S. Bötzel, and I. M. Eremin, Electronic correlations and superconducting instability in $\text{La}_3\text{Ni}_2\text{O}_7$ under high pressure, *Phys. Rev. B* **108**, L201121 (2023).
- [6] H. Sakakibara, N. Kitamine, M. Ochi, and K. Kuroki, Possible high T_c superconductivity in $\text{La}_3\text{Ni}_2\text{O}_7$ under high pressure through manifestation of a nearly-half-filled double-layer Hubbard model, [arXiv:2306.06039](https://arxiv.org/abs/2306.06039).
- [7] Y. Gu, C. Le, Z. Yang, X. Wu, and J. Hu, Effective model and pairing tendency in double-layer Ni-based superconductor $\text{La}_3\text{Ni}_2\text{O}_7$, [arXiv:2306.07275](https://arxiv.org/abs/2306.07275).
- [8] Y. Shen, M. Qin, and G.-M. Zhang, Effective bi-layer model Hamiltonian and density-matrix renormalization group study for the high- T_c superconductivity in $\text{La}_3\text{Ni}_2\text{O}_7$ under high pressure, *Chin. Phys. Lett.* **40**, 127401 (2023).
- [9] V. Christiansson, F. Petocchi, and P. Werner, Correlated electronic structure of $\text{La}_3\text{Ni}_2\text{O}_7$ under pressure, *Phys. Rev. Lett.* **131**, 206501 (2023).
- [10] D. A. Shilenko and I. V. Leonov, Correlated electronic structure, orbital-selective behavior, and magnetic correlations in double-layer $\text{La}_3\text{Ni}_2\text{O}_7$ under pressure, *Phys. Rev. B* **108**, 125105 (2023).
- [11] Z. Liu, H. Sun, M. Huo, X. Ma, Y. Ji, E. Yi, L. Li, H. Liu, J. Yu, Z. Zhang, Z. Chen, F. Liang, H. Dong, H. Guo, D. Zhong, B. Shen, S. Li, and M. Wang, Evidence for charge and spin order in single crystals of $\text{La}_3\text{Ni}_2\text{O}_7$ and $\text{La}_3\text{Ni}_2\text{O}_6$, *Sci. China: Phys., Mech. Astron.* **66**, 217411 (2023).
- [12] M. Nakata, D. Ogura, H. Usui, and K. Kuroki, Finite-energy spin fluctuations as a pairing glue in systems with coexisting electron and hole bands, *Phys. Rev. B* **95**, 214509 (2017).
- [13] P. A. Lee, N. Nagaosa, and X.-G. Wen, Doping a Mott insulator: Physics of high-temperature superconductivity, *Rev. Mod. Phys.* **78**, 17 (2006).
- [14] K.-W. Lee and W. E. Pickett, Infinite-layer LaNiO_2 : Ni^{1+} is not Cu^{2+} , *Phys. Rev. B* **70**, 165109 (2004).
- [15] D. Li, K. Lee, B. Y. Wang, M. Osada, S. Crossley, H. R. Lee, Y. Cui, Y. Hikita, and H. Y. Hwang, Superconductivity in an infinite-layer nickelate, *Nature (London)* **572**, 624 (2019).
- [16] G.-M. Zhang, Y.-F. Yang, and F.-C. Zhang, Self-doped Mott insulator for parent compounds of nickelate superconductors, *Phys. Rev. B* **101**, 020501(R) (2020).
- [17] Y.-F. Yang and G.-M. Zhang, Self-doping and the Mott-Kondo scenario for infinite-layer nickelate superconductors, *Front. Phys.* **9**, 801236 (2022).
- [18] P. Blaha, K. Schwarz, G. K. H. Madsen, D. Kvasnicka and J. Luitz, *WIEN2k, An Augmented Plane Wave + Local Orbitals Program for Calculating Crystal Properties* (Karlheinz Schwarz, Technische Universität Wien, Austria, 2001).
- [19] P. Blaha, K. Schwarz, F. Tran, R. Laskowski, G. K. H. Madsen, and L. D. Marks, WIEN2k: An APW+lo program for calculating the properties of solids, *J. Chem. Phys.* **152**, 074101 (2020).
- [20] A. Georges, G. Kotliar, W. Krauth, and M. J. Rozenberg, Dynamical mean-field theory of strongly correlated fermion systems and the limit of infinite dimensions, *Rev. Mod. Phys.* **68**, 13 (1996).
- [21] V. I. Anisimov, A. I. Poteryaev, M. A. Korotin, A. O. Anokhin, and G. Kotliar, First-principles calculations of the electronic structure and spectra of strongly correlated systems: Dynamical mean-field theory, *J. Phys.: Condens. Matter* **9**, 7359 (1997).
- [22] A. I. Lichtenstein and M. I. Katsnelson, *Ab initio* calculations of quasiparticle band structure in correlated systems: LDA++ approach, *Phys. Rev. B* **57**, 6884 (1998).
- [23] G. Kotliar, S. Y. Savrasov, K. Haule, V. S. Oudovenko, O. Parcollet, and C. A. Marianetti, Electronic structure calculations with dynamical mean-field theory, *Rev. Mod. Phys.* **78**, 865 (2006).
- [24] K. Held, O. K. Andersen, M. Feldbacher, A. Yamasaki, and Y. F. Yang, Bandstructure meets many-body theory: The LDA+DMFT method, *J. Phys.: Condens. Matter* **20**, 064202 (2008).
- [25] K. Haule, C.-H. Yee, and K. Kim, Dynamical mean-field theory within the full-potential methods: Electronic structure of CeIrIn_5 , CeCoIn_5 , and CeRhIn_5 , *Phys. Rev. B* **81**, 195107 (2010).
- [26] V. I. Anisimov, I. A. Nekrasov, D. E. Kondakov, T. M. Rice, and M. Sigrist, Orbital-selective Mott-insulator transition in $\text{Ca}_{2-x}\text{Sr}_x\text{RuO}_4$, *Eur. Phys. J. B* **25**, 191 (2002).
- [27] M. Vojta, Orbital-selective Mott transitions: Heavy fermions and beyond, *J. Low Temp. Phys.* **161**, 203 (2010).
- [28] J. H. Shim, K. Haule, and G. Kotliar, Modeling the localized-to-itinerant electronic transition in the heavy fermion system CeIrIn_5 , *Science* **318**, 1615 (2007).
- [29] Y. Xu, Y. Sheng, and Y.-F. Yang, Mechanism of the insulator-to-metal transition and superconductivity in the spin liquid candidate NaYbSe_2 under pressure, *npj Quantum Mater.* **7**, 21 (2022).
- [30] K. Momma and F. Izumi, VESTA 3 for three-dimensional visualization of crystal, volumetric and morphology data, *J. Appl. Crystallogr.* **44**, 1272 (2011).
- [31] A. Kokalj, XCrySDen – a new program for displaying crystalline structures and electron densities, *J. Mol. Graph. Model.* **17**, 176 (1999).
- [32] J. P. Perdew, K. Burke, and M. Ernzerhof, Generalized gradient approximation made simple, *Phys. Rev. Lett.* **77**, 3865 (1996).
- [33] H. Chen, A. Hampel, J. Karp, F. Lechermann, and A. Millis, Dynamical mean field studies of infinite layer nickelates: Physics results and methodological implications, *Front. Phys.* **10**, 835942 (2022).
- [34] M. Golalikhani, Q. Lei, R. U. Chandrasena, L. Kasaei, H. Park, J. Bai, P. Orgiani, J. Ciston, G. E. Sterbinsky, D. A. Arena, P. Shafer, E. Arenholz, B. A. Davidson, A. J. Millis, A. X. Gray, and X. X. Xi, Nature of the metal-insulator transition in few-unit-cell-thick LaNiO_3 films, *Nat. Commun.* **9**, 2206 (2018).
- [35] K. Haule, Quantum Monte Carlo impurity solver for cluster dynamical mean-field theory and electronic structure

- calculations with adjustable cluster base, *Phys. Rev. B* **75**, 155113 (2007).
- [36] M. Jarrell and J. E. Gubernatis, Bayesian inference and the analytic continuation of imaginary-time quantum Monte Carlo data, *Phys. Rep.* **269**, 133 (1996).
- [37] M. T. Czyżyk and G. A. Sawatzky, Local-density functional and on-site correlations: The electronic structure of La_2CuO_4 and LaCuO_3 , *Phys. Rev. B* **49**, 14211 (1994).
- [38] K. Haule, Exact double counting in combining the dynamical mean field theory and the density functional theory, *Phys. Rev. Lett.* **115**, 196403 (2015).
- [39] J. Mravlje, M. Aichhorn, T. Miyake, K. Haule, G. Kotliar, and A. Georges, Coherence-incoherence crossover and the mass-renormalization puzzles in Sr_2RuO_4 , *Phys. Rev. Lett.* **106**, 096401 (2011).
- [40] K. Haule and G. Kotliar, Coherence-incoherence crossover in the normal state of iron oxypnictides and importance of Hund's rule coupling, *New J. Phys.* **11**, 025021 (2009).
- [41] L. de' Medici, G. Giovannetti, and M. Capone, Selective Mott physics as a key to iron superconductors, *Phys. Rev. Lett.* **112**, 177001 (2014).
- [42] X. Wan, V. Ivanov, G. Resta, I. Leonov, and S. Y. Savrasov, Exchange interactions and sensitivity of the Ni two-hole spin state to Hund's coupling in doped NdNiO_2 , *Phys. Rev. B* **103**, 075123 (2021).
- [43] B. Kang, C. Melnick, P. Semon, S. Ryee, M. J. Han, G. Kotliar, and S. Choi, Infinite-layer nickelates as $\text{Ni-}e_g$ Hund's metals, *npj Quantum Mater.* **8**, 35 (2023).
- [44] Z. Liu, M. Huo, J. Li, Q. Li, Y. Liu, Y. Dai, X. Zhou, J. Hao, Y. Lu, M. Wang, and H.-H. Wen, Electronic correlations and energy gap in the bilayer nickelate $\text{La}_3\text{Ni}_2\text{O}_7$, [arXiv:2307.02950](https://arxiv.org/abs/2307.02950).
- [45] S. A. Hartnoll and A. P. Mackenzie, Planckian dissipation in metals, *Rev. Mod. Phys.* **94**, 041002 (2022).
- [46] B. Keimer, S. A. Kivelson, M. R. Norman, S. Uchida, and J. Zaanen, From quantum matter to high-temperature superconductivity in copper oxides, *Nature (London)* **518**, 179 (2015).
- [47] I. Božović and J. Levy, Pre-formed Cooper pairs in copper oxides and LaAlO_3 - SrTiO_3 heterostructures, *Nat. Phys.* **16**, 712 (2020).
- [48] Y.-F. Yang, G.-M. Zhang, and F.-C. Zhang, Interlayer valence bonds and two-component theory for high- T_c superconductivity of $\text{La}_3\text{Ni}_2\text{O}_7$ under pressure, *Phys. Rev. B* **108**, L201108 (2023).
- [49] Q. Qin and Y. Yang, High- T_c superconductivity by mobilizing local spin singlets and possible route to higher T_c in pressurized $\text{La}_3\text{Ni}_2\text{O}_7$, *Phys. Rev. B* **108**, L140504 (2023).
- [50] W. W. Warren, R. E. Walstedt, G. F. Brennert, R. J. Cava, R. Tycko, R. F. Bell, and G. Dabbagh, Cu spin dynamics and superconducting precursor effects in planes above T_c in $\text{YBa}_2\text{Cu}_3\text{O}_{6.7}$, *Phys. Rev. Lett.* **62**, 1193 (1989).
- [51] T. Yoshida, M. Hashimoto, S. Ideta, A. Fujimori, K. Tanaka, N. Mannella, Z. Hussain, Z.-X. Shen, M. Kubota, K. Ono, S. Komiya, Y. Ando, H. Eisaki, and S. Uchida, Universal versus material-dependent two-gap behaviors of the high- T_c cuprate superconductors: Angle-resolved photoemission study of $\text{La}_{2-x}\text{Sr}_x\text{CuO}_4$, *Phys. Rev. Lett.* **103**, 037004 (2009).